MEASUREMENT OF CHERENKOV RINGS WITH MULTIANODE PHOTOMULTIPLIERS

S.Korpar[1,2], R.Pestotnik[1], P.Križan[1,3], A.Gorišek[1], A.Stanovnik[1,4]

[1] *Jožef Stefan Institute, Ljubljana, Slovenia*

[2] *Faculty of Chemistry and Chemical Engineering, University of Maribor, Slovenia*

[3] *Faculty of Mathematics and Physics, University of Ljubljana, Slovenia*

[4] *Faculty of Electrical Engineering, University of Ljubljana, Slovenia*

November 27, 2013

Abstract

The present paper describes a laboratory course to be held at the ICFA 2010 Instrumentation School in Bariloche, Argentina. It is a continuation and upgrade of similar courses held in Itacuruça, Brasil in 2003 [1], in Istanbul in 1999 and 2002 and in Faure, South Africa in 2001. The main purpose of this exercise is to introduce the student to the Ring Imaging CHerenkov technique. The student will work with multianode photomultipliers (Hamamatsu, R5900-M16 and R5900-L16 PMT's), with which measurements requiring position sensitive detection of single photons will be performed. The first exercise is a measurement of the diffraction pattern by counting individual photons passing through a slit, and the second is a measurement of Cherenkov rings produced by cosmic muons in an aerogel radiator.

1 Introduction

Photomultiplier tubes (PMTs), or photomultipliers (PMs) for short, are sensitive detectors of weak light signals capable of detecting even single photons [2, 3]. The photomultiplier consists of an evacuated glass vessel containing a photocathode, from which incident photons may eject an electron, and a system of electrodes (dynodes) in which this photoelectron is multiplied to give a measurable electrical signal at the anode. The photocathode, the dynodes and the anode have leads through the glass to the outside of the vessel, enabling connections of high voltage and allowing the signals to be further processed by suitable electronics. The photomultiplier is thus plugged into a photomultiplier base, which consists of a resistor chain providing appropriate voltages for the dynodes and a load resistor, on which the signal

appears. In some cases, potentiometers are provided for adjusting the voltage on the electrodes for focusing the photoelectrons to the first dynode and capacitors or Zener diodes to stabilize the voltage on the last dynodes in case of high rate and high gain operation (Fig. 1).

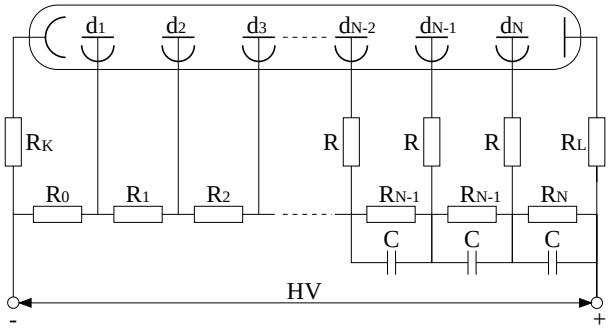

Figure 1: Voltage divider.

An important parameter of a photomultiplier is the quantum efficiency (QE), defined as the ratio of the number of photoelectrons ejected from the photocathode to the number of photons incident on the photomultiplier. Clearly, this parameter is a function of the energy (or wavelength) of the incident photons and is a product of the probability for the photoelectric effect and the probability for the electron to escape from the photocathode. The most common photocathode materials are semiconductors containing alkali elements. The quantum efficiency QE(λ) is connected to the photocathode radiant sensitivity S(λ), which is defined as the photocathode current divided by the incident photon power:

$$S(\lambda) = QE(\lambda)\frac{e_0\lambda}{hc}$$

The quantum efficiency is cut off on the low energy side by the vanishing probability for the photoelectron to escape into the vacuum and on the high energy side by photon absorption in the PM glass window.

The photoelectrons ejected from the photocathode are focused to the first dynode, where they eject more electrons. The electron multiplication is given by the secondary emission factor, which depends on the incident electron energy as well as on the dynode material. Usually, there are several dynodes (10 to 12) leading to an overall amplification of about 10^6 to 10^7.

In experimental physics, photomultipliers are most often used as detectors of scintillations, which charged particles, neutrons or gamma rays produce when depositing some or all of their energy in special scintillating materials. PMs may also be used as position sensitive detectors of single photons, especially for the Ring Imaging Cherenkov (RICH) counters in high energy physics experiments [4, 5, 6, 7].

The present laboratory course will introduce two such photomultiplier tubes produced by Hamamatsu Photonics K.K.; the R5900-M16 and the R5900-L16 multianode photomultipliers.

2 Position sensitive photomultipliers

The R5900 series M16 and L16 multianode photomultipliers are shown in Fig. 2. The M16 is divided into 4 x 4 = 16 anode outputs, each covering a pad size of 4.5 x 4.5 mm^2. The L16 anode, on the other hand, is divided into 16 strips of 16 mm length and 1 mm pitch. The exact dimensions of the photomultipliers and the locations of the electrode pin connectors are given in the data sheets [8].

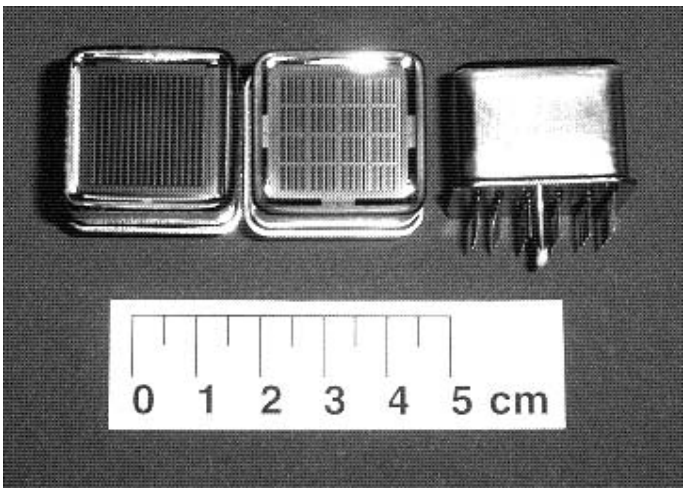

Figure 2: Hamamatsu multianode photomultipliers (L16, M16, M16 from left to right).

The quantum efficiency and the radiant sensitivity given by the manufacturer for L16 photomultipliers are shown in Fig. 3. It seems that allowance has to be made for an additional efficiency factor due to less than perfect collection and transmission ($\sim$80%) of the photoelectrons by the dynode system [5].

The dynode system in these multianode photomultipliers differs considerably from those in conventional photomultipliers. It consists of foils with specially shaped perforations or channels. On the walls of these channels, secondary emission takes place thus multiplying the number of electrons (Fig. 4). With 10-12 such dynode foils, gains above 10^6 are reached. The anode dark current is mainly below 200 nA [8]. Attention must be paid not to exceed the maximum allowed voltage of 900 V for L16 and 1000 V for M16 PMT and the maximum allowed current of 0.01 mA [8].

Of special interest e.g. in Cherenkov ring imaging is the position resolution, which is mainly given by the anode pad size. The cross-talk to adjacent channels is small and the response across the photocathode surface seems to be uniform to the level of some 10% [5, 8].

For the M16 photomultipliers, measurements have been made of single photoelectron pulse height distributions showing a well resolved single electron peak corresponding to a plateau on the rate-versus-voltage curve [5]. Tests with rates of 3 MHz/channel during 30 days [5] and two years of experience with the HERA-B

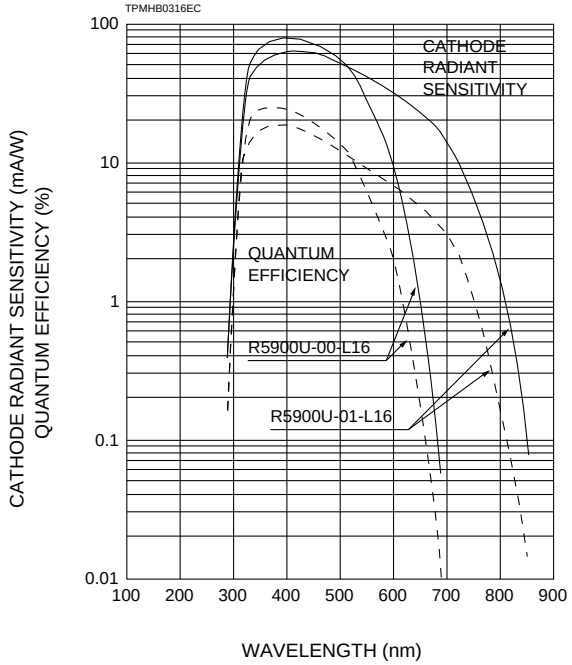

Figure 3: Typical spectral response of L16 PMT [8].

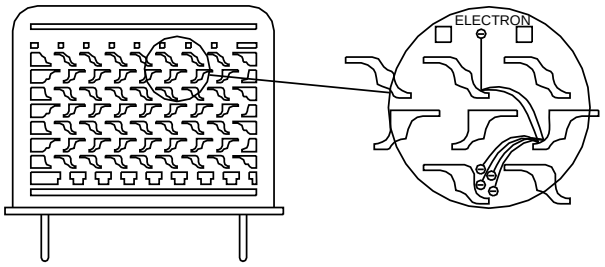

Figure 4: Metal channel type PMT [9].

photon detector [6], show that these photomultipliers operate smoothly even in otherwise hostile environments as are characteristic of the new high energy colliders. According to specifications [8], the pulse rise time is 0.8 ns with a transit time spread of 0.3 ns, so they could also be used for timing purposes.

3 Experimental set-up

The exercise is divided into three parts. The first consists of measuring the high voltage plateau and the position dependence of the M16 count rate for a pencil beam. The second part consists of measuring Cherenkov rings with an array of sixteen M16 PMTs. The third part of this exercise represents a measurement of a diffraction pattern by counting single photons with the L16 position-sensitive photomultiplier.

3.1 M16 - HV plateau and position dependence of the count rate

The experimental set-up for measuring the M16 photomultiplier is shown in Fig. 5. Light from the LED source is collimated by two pinholes, defining an illuminated spot of about 0.5 mm diameter on the photocathode. The photomultiplier is plugged

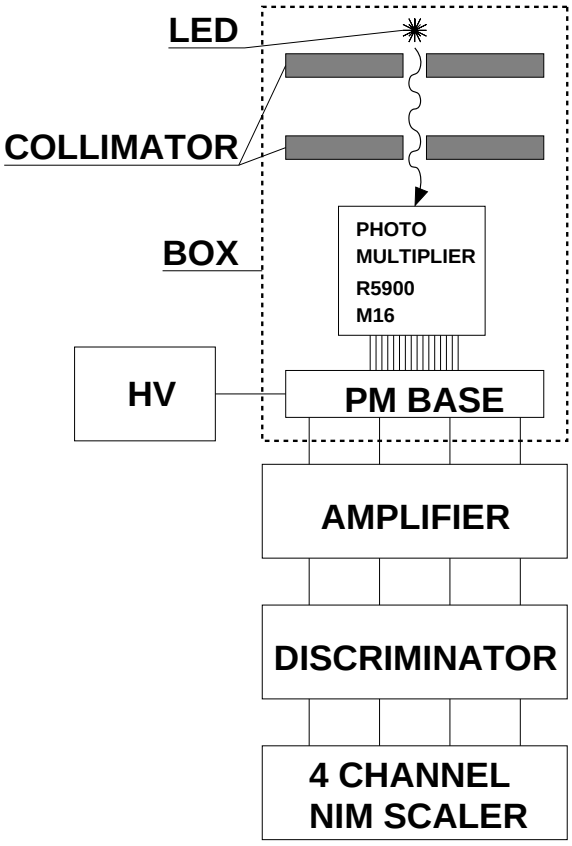

Figure 5: The experimental set-up for measuring the characteristics of M16 PMT.

into a PM base and both are enclosed in a light-tight box together with the light source and collimators. High voltage is provided by a HV power supply from which a cable leads to the PM base inside the light-tight box. Cables from four anode pads connect each signal first to an amplifier, then discriminator and finally to a scaler. The plate on which the PMT is fastened, may be displaced in a direction transverse to the light beam by means of a screw thread (1 mm/turn), which could be operated from the outside of the box. The height of the beam is set in order to be centered on one of the four rows with four pads. After observing the set-up the box is closed and the count rate at given threshold is recorded as a function of high voltage (see Fig.6). The voltage is then set on the plateau and count rates of the four pads are measured as a function of the PM position relative to the light spot (Fig.7). From the results of this measurement one may study the position resolution, the cross talk between adjacent pads, the uniformity of pad response and the response variation

across a given pad, which reflects the structure of the dynode channels, as also seen in Fig. 2.

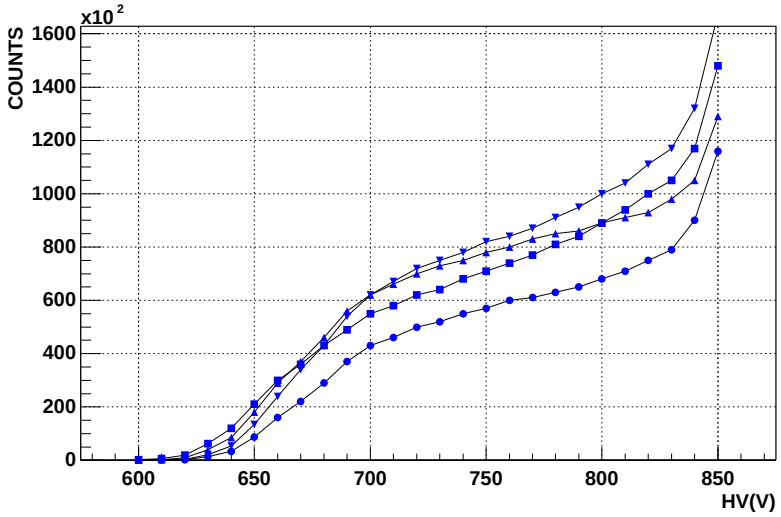

Figure 6: Plateau curves for 4 channels of the M16 PMT.

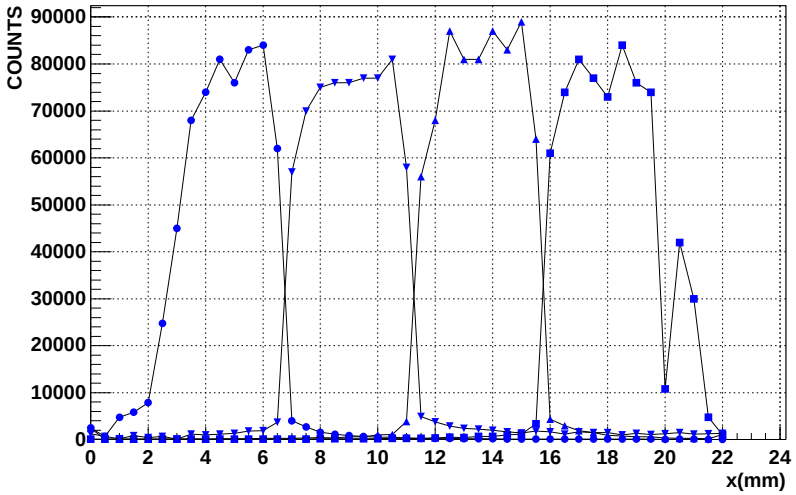

Figure 7: Count rate on 4 channels of the M16 PMT depending on the light spot position.

3.2 Array of M16 PMT's - Cherenkov rings

When the velocity $v = \beta c$ of a charged particle in a medium exceeds the speed of light c/n in that medium (c is the speed of light in vacuum and n is the refractive index of the medium), the particle emits light at an angle with respect to it's direction of motion. This Cherenkov angle is determined by the relation

$$\cos\theta_c = \frac{1}{\beta n}$$

and the threshold velocity for emission of Cherenkov light is at $\beta_{th} = 1/n$.

With a position sensitive detector of single photons, one may detect a Cherenkov ring image [10], from which the Cherenkov angle and thus the particle velocity may be determined. As the particle momentum is measured by other components of a detector system, one may use the velocity measurement to calculate the particle mass. Thus, Cherenkov detectors are usually refered to as particle identification devices. Most large detector systems operating at the high energy accelerators and colliders, include such a Ring Imaging Cherenkov detector (RICH) [11]. In the literature [10] we find that the number of detected photons is given by:

$$N = N_0 \cdot L \cdot \sin^2\theta_c.$$

N_0 is a figure of merit of the particular Cherenkov detector, which depends mainly on the efficiency of photon detection and the loss of photons between emission and detection. L is the length of the radiator and θ_c is the Cherenkov angle.

In the present exercise, we shall measure the Cherenkov photons radiated by high energy muons in an aerogel radiator. The muons are produced by cosmic rays in the upper layers of the atmosphere so are mainly incident from above onto the apparatus shown in Fig. 8. The muon first gives a trigger signal in a scintillation counter and then enters two, 2 cm thick aerogel layers ($n_1 = 1.0485$, $n_2 = 1.0619$), where a $\beta \simeq 1$ muon would radiate Cherenkov photons at $\theta_c = \arccos(1/n) = 305(343)$ mrad. The Cherenkov photons are refracted into air and are detected by the photon detector lying $\simeq$16 cm below the aerogel radiator entrance surface. The hits are distributed on the circumference of a ring of aproximately 5 cm radius (for $\beta \simeq 1$ particles). The radiator thickness leads to an uncertainty in the emission point, which translates into a $\approx$7 mm uncertainty in the hit position on the photon detector. This uncertainty and the shortage of readout channels resulted in four adjacent anode pads of the M16 PMT being connected into one 9×9 mm^2 pixel. The PMT array consists of sixteen M16 PMT's on a 30×30 mm^2 grid, so the geometrical acceptance of the photocathodes (18×18 mm^2) is 36 %. From this geometrical acceptance and the photocathode quantum efficiency ($\simeq$ 20% over $\Delta E \simeq 1$ eV), we estimate the figure of merit to be $N_0 \sim 15$ cm^{-1}. One may thus expect on average about 3 detected Cherenkov photons per full muon ring. As the number of photons is distributed statistically, a larger number (say 5 or 6) will be occasionally detected, allowing an estimate of the ring radius and thus the charged particle velocity.

The PMT anode signals are led through a discriminator to a 64 channel multihit TDC unit (CAEN V673A) (Fig. 8). The TDC is read out through the VME system into the computer (using WIENER PCI-VME interface), where appropriate algorithms reconstruct the hit maps displaying the Cherenkov ring images.

In Fig. 9 six events with high number of Cherenkov photons reconstructed are shown. They were taken at the ICFA Instrumentation School in Istanbul in 2002.

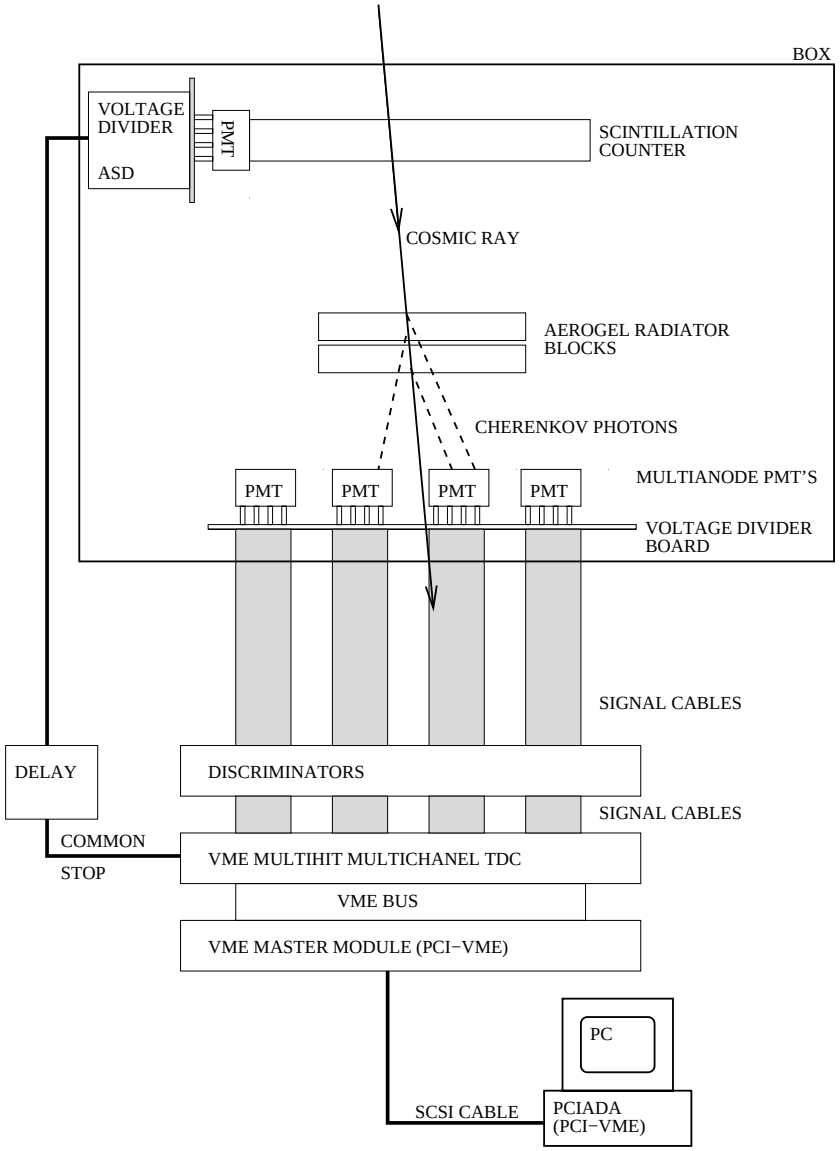

Figure 8: RICH counter for cosmic muons: the set-up.

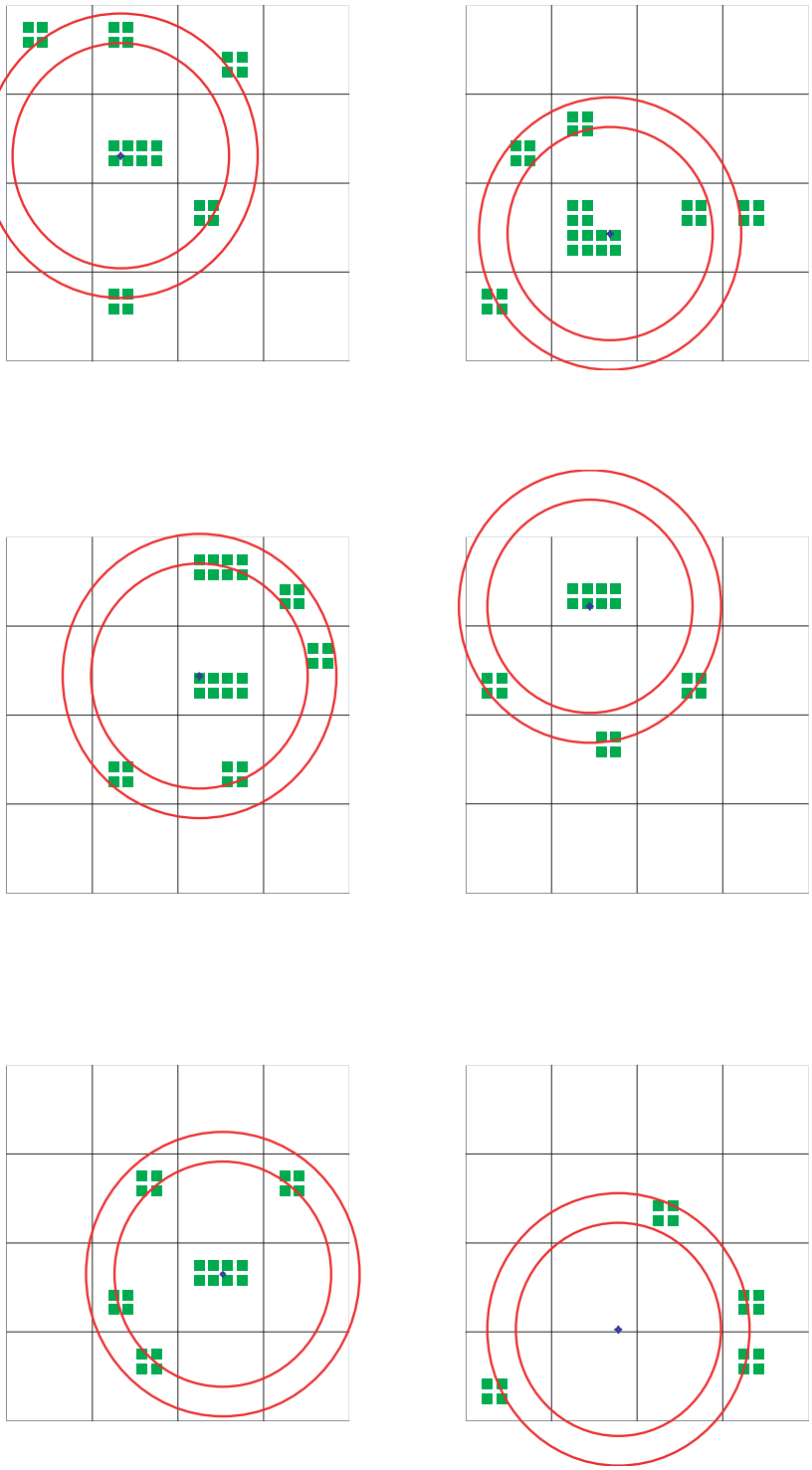

Figure 9: Reconstructed hits on the photon detector as obtained with the setup in Fig. 8. Six events with high number of hits were selected. The two red circles define the maximal and minimal rings which correspond to Cherenkov photons irradiated at the beginning and at the end of the aerogel radiator, correspondingly. 2x2 PMT channels were connected together in one readout channel, to simplify the readout electronics.

3.3 L16 - Diffraction pattern

The schematic diagram of this experimental set-up is shown in Fig.9. The light source is a light emitting diode (Fig.10). This light is passed through a slit of width D, on which diffraction occurs. The diffraction pattern is given by

$$j(\vartheta) = j_0 \frac{\sin^2 \alpha}{\alpha^2}$$

where $\alpha = \frac{\pi D \sin \vartheta}{\lambda}$ and ϑ is the diffraction angle with respect to the beam direction. In terms of the distance x from the central maximum and the distance L between the slit and the photomultiplier, this angle is given by tg $\vartheta = x/L$ (see Fig. 12). The first minimum in the diffraction pattern occurs at $\sin \vartheta_{min} = \lambda/D$. Assuming that the diffraction angle ϑ_{min} is small, the x-position of the minimum will be given by $x_{min}/L = \lambda/D$. In the present exercise one measures the position of the minimum and thus determines the slit width $D = \lambda \cdot L/x_{min}$.

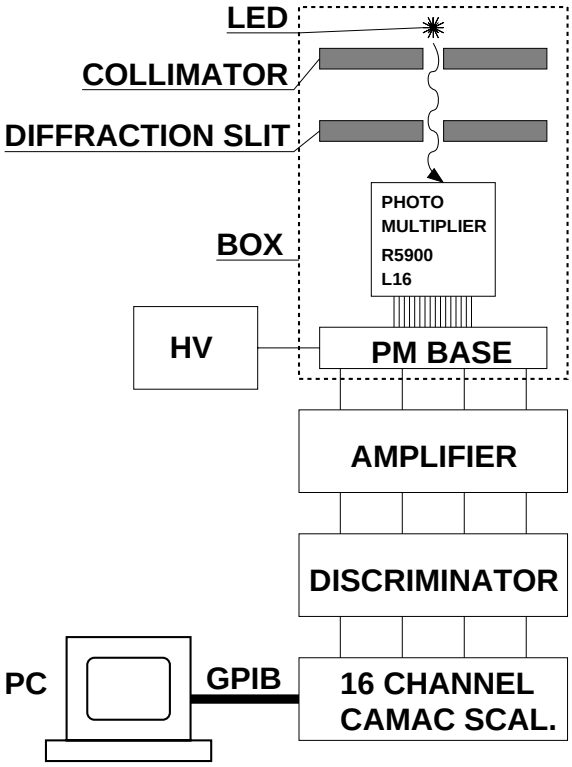

Figure 10: The experimental set-up for measuring diffraction with the L16 PMT.

From the 16 anode strips, the signals are led through amplifiers into CAMAC discriminators and then to a 16 channel CAMAC scaler. The counting time is set by removing the veto pulse on the discriminator. This is performed via a CAMAC input/output register and a NIM timing unit. The register and the scaler are connected via CAMAC and GPIB to a personal computer, which runs a data acquisition programme and displays the diffraction histogram. With the 16 channels at 1 mm

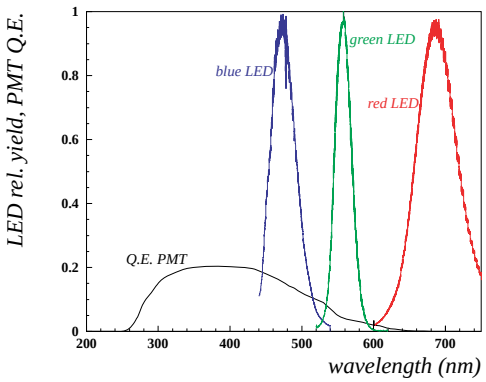

Figure 11: Spectra of three different LED sources.

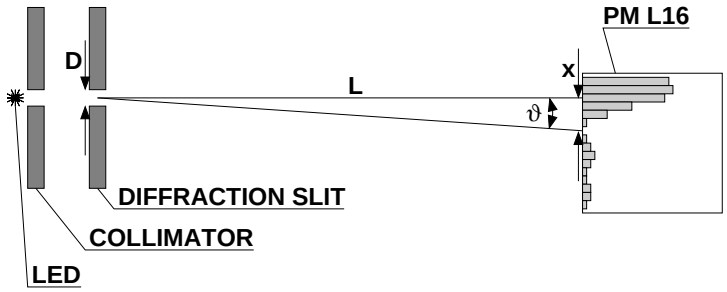

Figure 12: Geometric parameters for the diffraction measurement.

pitch only a 16 mm portion of the diffraction pattern could be measured simultaneously. In order to cover a broader range of diffraction angles, the photomultiplier may be displaced relative to the light beam by means of a screw thread (1mm/turn) operated from the outside of the light-tight box.

A diffraction pattern is first demonstrated by using a light beam from a laser pointer and slits made from razor blades. The slits are then inserted onto the rails in front of the light emitting diode, the distance L is measured and the box is closed. The high voltage on the PMT is set to approximately 800 V and the current through the LED is adjusted for an acceptable count rate. The diffraction pattern is then measured in at least two different positions of the PMT relative to the light beam and the results are appropriately connected. From the distribution (Fig. 13), one determines the position of the first minimum and then calculates the slit width D from the above equation. At this point the student may be reminded of the analogy between this experiment and the measurement of nuclear sizes by the so called diffraction scattering.

In this exercise, the pedagogical problem of wave-particle duality is stressed. With sufficiently low counting rate one may in principle simultaneously observe the count increment of individual channels and the appearance of the diffraction

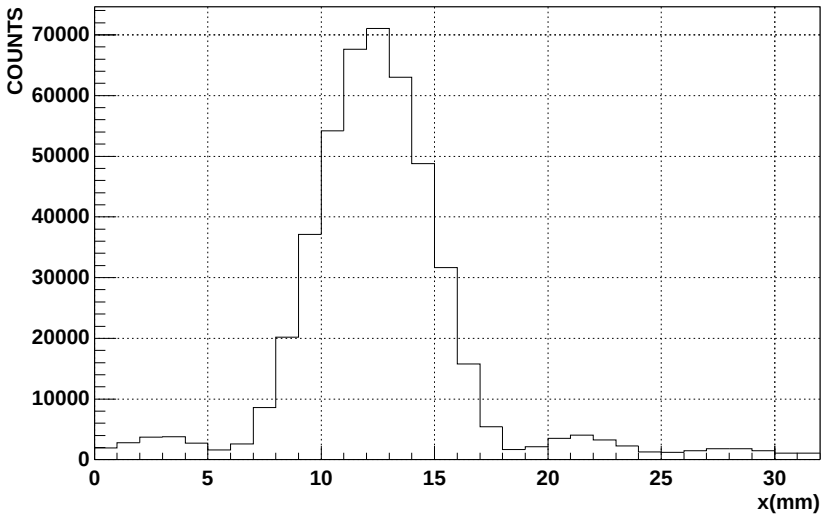

Figure 13: Measured diffraction distribution.

histogram (Fig. 13). The individual hit is a manifestation of the particle nature of the photon, while the diffraction distribution speaks of its wave properties.

Acknowledgment

We are grateful to Hamamatsu Photonics K. K. for donating some of the multianode photomultipliers used in the present laboratory course.

References

[1] S.Korpar, P.Križan, A.Gorišek, A.Stanovnik, Tests of a position sensitive photomultiplier and measurement of diffraction pattern by counting single photons, ICFA'99 Instrumentation School, Istanbul, Turkey, AIP Conference Proceedings, Vol. 536, p. 340-348

[2] G.F.Knoll, Radiation Detection and Measurement, John Wiley, 1989

[3] W.R.Leo, Techniques for Nuclear and Particle Physics Experiments, Springer-Verlag, 1987

[4] R. Debbe et al., In-beam tests of a Ring Imaging Cherenkov detector with a multianode photomultiplier read-out, Nucl. Inst. and Meth. in Phys. Res. **A362**(1995)253-260

[5] P.Križan et al., Tests of a Multianode PMT for the HERA-B RICH, Nucl. Inst. and Meth. in Phys. Res. **A394**(1997)27-34

[6] I.Arinõ et al., The HERA-B RICH, Nucl.Instr.Meth.Phys.Res.**A453**(2000)289-295

[7] N.Akopov et al., The HERMES dual radiator ring imaging Cherenkov detector, Nucl. Instr. Meth. Phys. Res. **A479**(2002)511-530

[8] Hamamatsu Photonics K.K., Data Sheet of R5900-L16 and Data Sheet of R5900-M16

[9] http://www.hpk.co.jp/hp2e/products/Etd/PDFfiles/PMThd6E.pdf

[10] E.Nappi, RICH detectors, ICFA'99 Instrumentation School, Istanbul, Turkey, AIP Conference Proceedings, Vol. 536, p. 60-86.

[11] Advances in Cherenkov Light Imaging Techniques and Applications, eds. A.Breskin, R.Chechik, T.Ypsilantis, Proceedings of the Third International Workshop on Ring Imaging Cherenkov Detectors (RICH98), Ein Gedi, Dead Sea, Israel, November 15 -20, 1998, Nucl. Instr. Meth. Phys. Res. **A433**(1999)